Electronics and Electrical Engineering

AIMS Electronics and Electrical Engineering, 9(1): 81–98.
DOI: 10.3934/electreng.2025005
Received: 18 October 2024
Revised: 06 December 2024
Accepted: 06 January 2025
Published: 14 January 2025

https://www.aimspress.com/journal/ElectrEng

Research article

Improved sliding mode control for induction motor based on twisting algorithm

Hadda Benderradji[1,*], Samira Benaicha[1] and Larbi Chrifi Alaoui[2]

[1] Electrical Engineering Department, LSPIE Laboratory, University Batna2, Batna, Algeria
[2] Laboratory LTI (EA, 3899), Univ of Picardie-Jules verne, France

*** Correspondence:** Email: h.benderradji@univ-batna2.dz.

Abstract: In this paper, the output feedback tracking issue of induction motors is resolved by applying the sliding mode approach. We designed and implemented two robust sliding mode (SM) techniques to achieve high-performance control of induction motor drive; the second-order sliding mode (SOSM) approach using the twisting algorithm was compared with the classical sliding mode control. The method of decoupling electromagnetic torque and rotor flux for the induction motor was derived from the rotor field orientation control in the synchronous reference frame. The objective of the proposed methods is to control the rotor speed and the square of the rotor flux separately, in order to obtain robust control against disturbances and parametric uncertainties, and at the same time minimize the chattering phenomenon—the most significant drawback in the actual implementation of this technique. The stability of the proposed first-order sliding mode control was confirmed using Lyapunov stability theory. The availability and effectiveness of the proposed techniques were demonstrated through experimental results. The comparison between the results of the two proposed methods shows that the second-order sliding mode control using the twisting algorithm not only guarantees the same robustness and dynamic performances of traditional first-order sliding mode control but also achieves the reduction of the chattering phenomenon.

Keywords: induction motor; sliding mode method; twisting algorithm; sliding manifold; chattering phenomenon

1. Introduction

Induction motors (IMs), which are used in industrial processes for variable speed and position control, have become more attractive in recent years because of their simplicity, lower cost, affordability, and easy maintenance needs. However, IM control has been a conceptually tough topic due to its complex dynamic characteristics, which are highly nonlinear and coupled as flux and electromagnetic torque [1,2]. Recent developments in power electronics with sophisticated control techniques have enabled the employment of electrical drives, particularly induction motors, in high-performance, variable-speed applications. In the literature, several methods for IM control have been studied, the most widely used being field-oriented control (FOC). In FOC, the rotor flux and torque that generate current components are decoupled to provide reaction properties akin to those of a direct current motor [3–7]. However, conventional strategies of FOC may struggle with parametric variations and uncertainty and be unable to provide the desired performance [8].

As a result, great effort has been expended on developing the performance and robustness of an induction motor's control approaches. An intriguing technique for controlling nonlinear systems is the sliding mode control, which is distinguished by its extreme simplicity and resilience to disturbances and parameter changes. This method drives the system state's trajectory toward a switching surface in the state space via discontinuous control [9]. The sliding mode control (SMC) has been used in combination with other methods as a model reference adaptive system (MRAS) [10] and with fuzzy logic technique and indirect field-oriented control (IFOC) techniques [11].

In spite of its advantages, there is a drawback associated with this method—the chattering phenomenon. Chattering can induce torque pulsation and current harmonics among other undesired consequences by exciting the system's high-frequency unmodeled dynamics. To overcome this drawback, many advanced methods have been developed, and several techniques for robust chattering reduction are dependent on modifying the switching functions [12–14]. While high-frequency chattering may be easily reduced or eliminated by using the saturation function, this will inevitably result in a loss of some robustness against load disturbances and uncertainties. However, the majority of steady-state errors will still be present.

To minimize the steady-state error and specify the integral sliding mode controller, an integral sliding surface is a recommended technique [14–20]. Steady-state error (SSE) in pseudo-sliding modes can be avoided by using a pseudo-sliding mode control, as introduced in [20], in which smooth functions replace the switching function with the inclusion of integral terms. This turns the system into pseudo-sliding modes, resulting in SSEs. On the other hand, by adding an integral term to the surface, the system can be vulnerable to windup. This causes the system response to significantly overshoot and exhibit undesired oscillations. Using a switching sigmoid function, authors in [21] suggested an integrated sliding mode controller with a novel anti-windup technique that has low overshoot and no steady-state inaccuracy.

Another class of SMC approaches to attenuate the chattering and achieve robust control is called high-order SMC [22–27]. Several suggested approaches are used to construct a variety of novel second-order sliding mode controllers (SOSMC), including the twisting algorithm [28,29] and the super twisting algorithm [30–32]. It should be mentioned that SOSM algorithms require bounded uncertainties in sliding mode dynamics because state variables are constantly related to uncertainties. This means that state variables should also be bounded, even though determining the domain of attraction is usually not easy [25,33].

This work aims to compare two sliding mode control techniques applied to IM—a classical SMC and a second-order SMC—using the twisting algorithm, whose aim is to reduce chattering. The findings of the experiment are examined and presented.

The structure of the paper is as follows: Section 2 presents the induction motor model in the synchronous reference frame, and the field-oriented model is explained. In Section 3, the classical sliding mode control theory for a nonlinear system is briefly reviewed. The two proposed controls are described and developed in Section 4. In Section 5, experimental results of the implemented controls are presented to examine the effectiveness and compare their performance. Section 6 provides a summary of the study's main conclusions.

2. Induction motor model of field-oriented flux

Accurate mathematical modeling is essential to effectively control the various operating modes of IMs. The following expressions represent the mathematical model of the IM in terms of stator current and rotor flux in the synchronous reference frame [2]:

$$\begin{aligned}
\frac{di_{sd}}{dt} &= -\delta\, i_{sd} + \omega_s\ i_{sq} + \alpha\,\beta\,\phi_{rd} + p\beta.\Omega.\phi_{rq} + \frac{1}{\sigma L_s}u_{sd}\\
\frac{di_{sq}}{dt} &= -\omega_s\ i_{sd} - \delta\, i_{sq} - \beta p\Omega\,\phi_{rd} + \alpha\,\beta\,\phi_{rq} + \frac{1}{\sigma L_s}u_{sq}\\
\frac{d\phi_{rd}}{dt} &= \alpha M i_{sd} - \alpha\phi_{rd} + (\omega_s - p\Omega).\phi_{rq}\\
\frac{d\phi_{rq}}{dt} &= \alpha M i_{sq} - (\omega_s - p\Omega)\phi_{rd} - \alpha\phi_{rq}
\end{aligned} \tag{1}$$

The mechanical modeling part of the system is given by:

$$\frac{d\Omega}{dt} = \mu\left(\phi_{rd} i_{sq} - \phi_{rq} i_{sd}\right) - \frac{T_L}{j} - \frac{F}{j}\Omega \tag{2}$$

Where the electromagnetic torque T_e is given by:

$$T_e = \mu\left(\phi_{rd} i_{sq} - \phi_{rq} i_{sd}\right) \tag{3}$$

With:

$$\sigma = 1 - \frac{M^2}{L_s L_r}, \qquad b = \frac{1}{\sigma L_s}, T_r = \frac{L_r}{R_r}, \alpha = \frac{1}{T_r}, \qquad \beta = \frac{M}{\sigma\, L_s L_r},$$

$$\mu = \frac{pM}{j\, L_r}, \delta = \frac{M^2 R_r}{\sigma L_s L_r^2} + \frac{R_s}{\sigma L_s}\ ,\ I = \begin{bmatrix}1 & 0\\ 0 & 1\end{bmatrix},\ J = \begin{bmatrix}0 & -1\\ 1 & 0\end{bmatrix}$$

Where ϕ_{rd}, ϕ_{rq} are the rotor flux components, and i_{sd}, i_{sq} are the stator currents. $u_s = \left[u_{sd}, u_{sq}\right]^T$ is the control vector. T_L is the load torque, ω is the mechanical frequency of rotor speed, ωs is the electrical stator frequency speed, σ is a total leakage factor, and T_L is the rotor time constant. R_s and R_r denote stator and rotor resistance, L_s and L_r are the stator and rotor self-inductance, M is mutual inductance, p is the number of pole pairs, j is the moment of inertia, and F is the friction coefficient.

A rotor field orientation in the synchronous reference frame (d, q) is achieved if we let $\phi_{rq} = 0$ and $\phi_{rd} = \phi_r$, [3]. The IM model, after field-oriented transformation, becomes:

$$\dot{x} = f(x) + g(x)u_s \tag{4}$$

With:

$$f(x) = \begin{bmatrix} f_1(x) \\ f_2(x) \\ f_3(x) \\ f_4(x) \end{bmatrix} = \begin{bmatrix} -\delta i_{sd} + \omega_s i_{sq} + \alpha\beta\phi_{rd} \\ -\omega_s i_{sd} - \delta i_{sq} - \beta p\Omega\phi_{rd} \\ \alpha M i_{sd} - \alpha\phi_{rd} \\ \mu\phi_{rd} i_{sq} - \frac{F}{j}\Omega - \frac{C_r}{j} \end{bmatrix}, \quad g(x) = \begin{bmatrix} b & 0 & 0 & 0 \\ 0 & b & 0 & 0 \end{bmatrix}^T$$

The components of the function *f*(x) are nonlinear functions, $x = [i_{sd} \ i_{sq} \ \phi_r \ \Omega]^T$ is the state space vector, and the control vector u_s is defined by $[u_{sd} \ u_{sq}]^T$. The objective of vector control is to enable decoupling control of torque and rotor flux. After orientation of the flux, the electromagnetic torque becomes:

$$T_e = \mu \phi_r i_{sq} \tag{5}$$

Additionally, the direct stator current component may be used to reconstruct the rotor flux using the third equation in Eq (4):

$$\hat{\phi}_r = \frac{M}{T_r s + 1} i_{sd} \tag{6}$$

Where s is the Laplace operator. According to (5) and (6), we obtain two independent actions: the stator component i_{sd} controls the flux, and i_{sq} controls the torque, achieving the classical direct FOC control objective [3].

The synchronous rotating frame angle θ_s can be determined by integrating the synchronous angular frequency ω_s as below:

$$\hat{\theta}_s = \int \hat{\omega}_s dt = \int (\hat{\omega}_r + p\Omega) dt \tag{7}$$

The slip angular frequency ω_r is given by:

$$\hat{\omega}_r = \frac{\alpha M}{\hat{\phi}_r} i_{sq} \tag{8}$$

In the following section we will apply two techniques, the first-order and the second-order sliding mode, to control the IM.

3. Sliding mode control strategy

3.1. Problem formulation

Although a sliding mode method is known to be robust to disturbances and parametric uncertainties, one particular drawback in classical sliding mode techniques (first-order SM) is the chattering phenomena, which is essentially motion that oscillates around the sliding surface. To overcome this undesirable phenomenon, the higher-order sliding mode concept has been introduced

by Levant et al. [24].

Consider a dynamic system of the form:

$$\dot{x} = a(x) + b(x)u \tag{9}$$

$$S = S(x,t) \tag{10}$$

Where $x \in R^n, u \in R$ are the state and control input of system, *a(x), b(x)* are smooth functions, S is the smooth output function, and n is the dimension of the system.

Let the system be closed by some dynamical discontinuous feedback; we may construct consecutive total time derivatives, and the closed-system state-space variables' continuous functions are $S = \dot{S} = \ddot{S} = \cdots = S^{(r-1)}$. The fundamental objective is to establish a limited time convergence onto the so-called r-order sliding mode, which is composed locally of Filippov trajectories and is represented as the non-empty surface $S = \dot{S} = \ddot{S} = \cdots = S^{(r-1)} = 0$. Additionally, the regulation of the rth-order sliding mode achieves greater accuracy in terms of chattering [25].

However, because the chosen outputs have a relative degree equal to two with regard to S, a finite time convergence to S = 0 can only be accomplished using higher-order sliding modes. As it occurs, a first-order sliding mode controller would yield an asymptotic convergence. This finding serves as further justification for using a second-order sliding mode in addition to the chattering reduction. The twisting method is a popular example of a second-order algorithm. In general, the second-order sliding controller needs the sliding surface and its derivative to be made available and is determined by the equalities $S = \dot{S} = 0$. The purpose is to produce $\dot{S} = 0$ in finite time while keeping S on zero by discontinuous feedback control. For every limited input, system trajectories are meant to be indefinitely extendible in time, and the system is understood in the Filippov sense [34]. The dynamics of sliding function S may be characterized as follows:

$$\ddot{S} = A(x) + B(x)u \tag{11}$$

Where S and $\dot{S}$ are assumed to be measurable. This is accomplished by computing the second total time derivative of S along the trajectories of (9) under these conditions [25]: $A(x) = \ddot{S}\big|_{u=0}$ and $B(x) = \frac{\partial \dot{S}}{\partial u} \neq 0$, where the functions $A(x)$ and $B(x)$ are some unknown smooth functions satisfying the following conditions:

$$|A(x)| \leq C_0, \qquad K_m \leq B(x) \leq K_M \tag{12}$$

Where C_0, K_m, K_M are three positive coefficients. The uncertainties of the sliding mode dynamics of (10) are clearly bound by positive constants, implying that the state variables may also be confined. Then, (11) and (12) imply the following differential inclusion:

$$\ddot{S} = [-C_0\ ,\ C_0] + [K_m\ ,\ K_M]u \tag{13}$$

We suggest the twisting algorithm, created by A. Levant, which has an easy-to-use design and simple shape. This algorithm relies on appropriately switching control between two distinct values to ensure that the trajectories in the phase plane converge to the origin within a finite time [29]. The convergence of the twisting algorithm is ensured by a geometric progression that takes the shape of a spiral movement around the origin. The control law of the twisting algorithm is provided by:

$$u = \begin{cases} -\lambda_m sgn(S) & if\ \ S\dot{S} \leq 0 \\ -\lambda_M sgn(S) & if\ \ S\dot{S} > 0 \end{cases} \tag{14}$$

Where λ_m , λ_M are positive constants, with $0 < \lambda_m < \lambda_M$, , $K_m\lambda_M - C_0 > K_M\lambda_m + C_0$.

The twisting algorithm is well-suited for controlling systems with second-order dynamics or those requiring precision in higher-order derivatives, such as trajectory tracking in different applications. Introducing a twisting algorithm into sliding mode control (SMC) is primarily aimed at addressing limitations of traditional sliding mode control, such as chattering, while improving control performance and robustness.

The twisting algorithm offers finite-time convergence to the sliding surface compared to conventional SMC techniques that could only guarantee asymptotic convergence. This property is crucial in time-critical systems or applications requiring fast stabilization. The twisting algorithm achieves continuous convergence; it gets rid of abrupt control actions with smooth control updates and, by mitigating chattering, it decreases mechanical stress on actuators. By producing smoother control signals, the twisting algorithm improves overall system performance and lowers control input energy, making it desirable to several applications [28,33]. In practice, implementing the twisting algorithm is easy, but we need to obtain the first derivative of the switching surface.

4. Induction motor control by sliding mode method

4.1. First-order SM control of IM

The chosen sliding surface is defined by:

$$S(x) = ke + \dot{e}\,, \quad k > 0 \tag{15}$$

Such as:

$$(x) = \begin{bmatrix} s_\omega \\ s_\varphi \end{bmatrix},\ e = \begin{bmatrix} e_\omega \\ e_\varphi \end{bmatrix} = \begin{bmatrix} \Omega - \Omega_{ref} \\ \varphi - \varphi_{ref} \end{bmatrix},\ \varphi = \phi_{rd}^2,\ k = \begin{bmatrix} \mathrm{k}_1 & 0 \\ 0 & \mathrm{k}_2 \end{bmatrix}$$

Where e is the error between the measured rotor speed Ω, the estimated value of the square of the flux modulus φ, and their references Ω_{ref} and φ_{ref}.

For good tracking of speed and flux, it is important to make the surface invariant $\left(\dot{\mathrm{S}}(\mathrm{x}) = 0\right)$ and attractive $\left(S^T\dot{\mathrm{S}} < 0\right)$. The derivative of the surface gives:

$$\dot{S}(x) = k\dot{e} + \ddot{e} = Q(x) + R(x)u_s \tag{16}$$

$$\mathrm{Q(x)} = \begin{bmatrix} \mathrm{q}_1(\mathrm{x}) \\ \mathrm{q}_2(\mathrm{x}) \end{bmatrix},\ \mathrm{R(x)} = -\frac{\phi_{rd}}{\sigma \mathrm{L_s}} \begin{bmatrix} 0 & \mu \\ 2\alpha\mathrm{M} & 0 \end{bmatrix}$$

$$\mathrm{q}_1(\mathrm{x}) = (\mathrm{k}_1 - \tfrac{\mathrm{F}}{\mathrm{j}})\dot{\Omega} - \mathrm{k}_1\dot{\Omega}_{\mathrm{ref}} + \mu\left[\alpha\mathrm{M}\mathrm{i}_{\mathrm{sd}}\,\mathrm{i}_{\mathrm{sq}} - (\alpha+\delta)\phi_{\mathrm{rd}}\,\mathrm{i}_{\mathrm{sq}} - \omega_{\mathrm{s}}\phi_{\mathrm{rd}}\,\mathrm{i}_{\mathrm{sd}} - \mathrm{p}\beta\omega\varphi\right] - \tfrac{\dot{\mathrm{C}}_{\mathrm{r}}}{\mathrm{j}} - \ddot{\Omega}_{ref}$$

$$\mathrm{q}_2(\mathrm{x}) = \mathrm{k}_2\dot{\varphi} - \mathrm{k}_2\dot{\varphi}_{\mathrm{ref}} + 2\alpha\mathrm{M}\left[\alpha\mathrm{M}i_{sd}^2 - (3\alpha+\delta)\phi_{\mathrm{rd}}\,\mathrm{i}_{\mathrm{sd}} + \omega_{\mathrm{s}}\phi_{\mathrm{rd}}\,\mathrm{i}_{\mathrm{sq}}\right] + 2\alpha^2(\beta\mathrm{M}+2)\varphi - \ddot{\varphi}_{ref}$$

The surface $\mathrm{S} = 0$ is invariant if $\dot{\mathrm{S}} = 0$, where $Q(x) + R(x)u_{eq} = 0$, so we can therefore deduce the equivalent component as follows:

$$u_{eq} = -[R(x)]^{-1}Q(x) \tag{17}$$

The surface S becomes attractive if we choose u_{glis} in the following form:

$$u_{glis} = -[R(x)]^{-1}\left(\begin{bmatrix}\lambda_\Omega & 0\\ 0 & \lambda_\varphi\end{bmatrix}\begin{bmatrix}sng(s_\Omega)\\ sng(s_\varphi)\end{bmatrix}+\begin{bmatrix}k_\Omega s_\Omega\\ k_\varphi s_\varphi\end{bmatrix}\right) \tag{18}$$

λ_Ω, λ_φ, k_Ω, and k_φ are positive constants chosen such that:

$$\begin{cases}\lambda_\Omega \ and \ k_\Omega > |q_1(x)|\\ \lambda_\varphi \ and \ k_\varphi > |q_2(x)|\end{cases}$$

In sliding mode, Equation (15) becomes:

$$\begin{aligned}\dot{e}_\Omega &= -k_1 e_\Omega\\ \dot{e}_\varphi &= -k_2 e_\varphi\end{aligned} \tag{19}$$

From (19), the tracking errors in speed e_Ω and flux e_φ converge exponentially toward 0.

The sliding mode control law $u_s = u_{eq} + u_{glis}$ is given by:

$$u_s = -[R(x)]^{-1}\left(Q(x)+\begin{bmatrix}\lambda_\Omega & 0\\ 0 & \lambda_\varphi\end{bmatrix}\begin{bmatrix}sng(s_\Omega)\\ sng(s_\varphi)\end{bmatrix}+\begin{bmatrix}k_\Omega s_\Omega\\ k_\varphi s_\varphi\end{bmatrix}\right) \tag{20}$$

In practice, we encountered vibration problems hindering the proper functioning of the motor due to the chattering. For this, we replaced the sign function [sng(S)] of the discontinuous part of the control law of (20) with the saturation function (Sat), to avoid or at least lessen it. We define the following saturation function [12,24]:

$$Sat(S(x)) = \begin{cases} sgn(S) & if \ |S| > \varepsilon\\ \frac{S}{\varepsilon} & if \ |S| \le \varepsilon\end{cases} \tag{21}$$

Where ε is the boundary layer thickness.

Mitigating vibration problems caused by chattering by replacing the sign function Sng(S) with a saturation function Sat(S) is an effective strategy in control systems, particularly in sliding mode control (SMC). The continuous nature of Sat(S) within the boundary layer ε reduces high-frequency switching, minimizing mechanical vibrations and noise and improving actuator lifetime; this means that we can get softened control action near the switching surface.

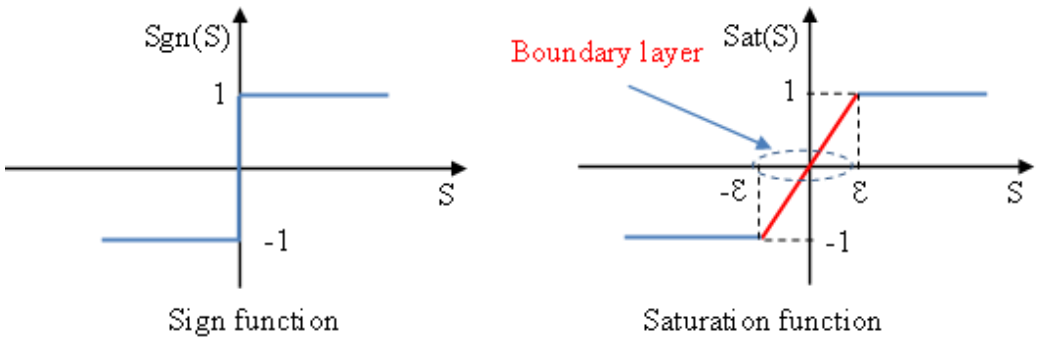

Figure 1. Discontinuous function Sng(S) and continuous function Sat(S).

The introduction of a boundary layer ε compromises the perfect tracking behavior of the sliding mode. If ε is too large, the system may exhibit steady-state error. Selecting an appropriate ε is critical; it should be large enough to avoid chattering but small enough to ensure accurate tracking within the desired response time. In practice, by judiciously adjusting the parameter ε, a compromise can be found between robustness, precision, and vibration reduction. This concept is widely used in industrial applications requiring precise and reliable control of motors [12,35]. There are several types of functions with different boundary layers, such as $\tanh\left(\frac{S}{\varepsilon}\right)$, $\frac{S}{S+\varepsilon}$, $\frac{2}{\pi}\text{atan}\left(\frac{S}{\varepsilon}\right)$, . . . etc.

4.1.1. Stability analysis

The suggested sliding mode controllers must meet the requirements of Lyapunov's stability theory in order to ensure the stability of the system. The selection of the positive Lyapunov's function is as follows:

$$V = \frac{1}{2}S^T S \tag{22}$$

The time derivative of V is that:

$$\dot{V} = \dot{S}^T S \tag{23}$$

Substituting (16) and (20) into (23), the derivative of Lyapunov function V becomes:

$$\dot{V} = \left((Q(x) - R(x)[R(x)]^{-1}(Q(x) + \lambda sng(S) + kS)\right).S \tag{24}$$

With: $\lambda = \begin{bmatrix}\lambda_\Omega & 0\\ 0 & \lambda_\varphi\end{bmatrix}$, $k = \begin{bmatrix}k_\Omega\\ k_\varphi\end{bmatrix}$

$$\dot{V} = -\lambda.S.sng(S) - kS^2 = -\lambda|S| - kS^2 < 0 \tag{25}$$

The stabilized system will occur when the attaining Lyapunov function criterion $\dot{V} < 0$ is met by the designed nonlinear sliding mode controller, as indicated by (20).

4.2. Second-order SM control of IM

We take into consideration the uncertain model of the asynchronous motor provided by the form in order to construct a control by second-order sliding modes that guarantees robust performance in the face of parametric changes and disturbances:

$$\dot{x} = f(x) + \Delta f(x) + (g(x) + \Delta g(x))u_s \tag{26}$$

Where $f(x)$ and $g(x)$ constitute the nominal parts, and Δf, Δg represents uncertainties such that:

$$\Delta f = [\Delta f_1 \quad \Delta f_2 \quad \Delta f_3 \quad \Delta f_4]^T,\ \Delta g = \begin{bmatrix}\Delta g_1 & 0 & 0 & 0\\ 0 & \Delta g_2 & 0 & 0\end{bmatrix}^T$$

The control vector is u_s so that $u_s \leq |u|_{max}$.

The relative degree of a system is the derivative number of the output to explicitly see the input (the command). To develop the control law according to the twisting algorithm, we choose the sliding surface S given by (27), such that the relative degree equals 2.

$$S = \begin{pmatrix} s_1 \\ s_2 \end{pmatrix} = \begin{pmatrix} \Omega - \Omega_{ref} \\ \varphi - \varphi_{ref} \end{pmatrix} \tag{27}$$

Substituting (26) in the second derivative of S, we obtain:

$$\ddot{S} = H(x) + G(x)u_s = \left(\hat{H}(x) + \Delta H\right) + (\hat{G}(x) + \Delta G)u_s \tag{28}$$

with:

$$H(x) = \begin{bmatrix} H_1(x) \\ H_2(x) \end{bmatrix} = \begin{bmatrix} \hat{H}_1(x) \\ \hat{H}_2(x) \end{bmatrix} + \begin{bmatrix} \Delta H_1 \\ \Delta H_2 \end{bmatrix}, G(x) = \begin{bmatrix} 0 & G_1(x) \\ G_2(x) & 0 \end{bmatrix} = \begin{bmatrix} 0 & \hat{G}_1(x) \\ \hat{G}_2(x) & 0 \end{bmatrix} + \begin{bmatrix} 0 & \Delta G_1 \\ \Delta G_2 & 0 \end{bmatrix}$$

$$\hat{H}_1(x) = \mu\left[\alpha M i_{sd} i_{sq} - (\alpha + \delta)\phi_{rd} i_{sq} - \omega_s \phi_{rd} i_{sd} - p\beta\omega\varphi\right] - \frac{\dot{C}_r}{j} - \frac{F}{j}\dot{\Omega} - \ddot{\Omega}_{ref}$$

$$\Delta H_1 = \mu[\phi_{rd}\Delta f_2 + i_{sq}\Delta f_3] - F\Delta f_4 + \dot{\Delta f_4}$$

$$\hat{H}_2(x) = 2\alpha M\left[\alpha M i_{sd}^2 - (3\alpha + \delta)\phi_{rd} i_{sd} + \omega_s \phi_{rd} i_{sq}\right] + 2\alpha^2(\beta M + 2)\varphi - \ddot{\varphi}_{ref}$$

$$\Delta H_2 = \Delta f_3\left(4\alpha M i_{sd} - 6\alpha\phi_{rd} + \Delta f_3\right) + 2\alpha M\phi_{rd}\Delta f_1 + 2\phi_{rd}\dot{\Delta f_3}$$

$$\hat{G}_1(x) = -\mu b\phi_{rd}, \hat{G}_2(x) = 2\alpha M b\phi_{rd}, \qquad \Delta G_1 = \mu\phi_{rd}\Delta g_1, \qquad \Delta G_2 = 2\alpha M\phi_{rd}\Delta g_2$$

It is assumed that $|\Delta H_1|$, $|\Delta H_2|$, $|\Delta G_1|$ and $|\Delta G_2|$ are limited. The load torque T_L must also be bound as well as its first derivative.

By using the twisting method, the system's trajectories are forced to develop on the surface S after a finite amount of time, creating a second-order sliding regime that results in $S = \dot{S} = 0$.

The proposed final control using state space feedback is given by:

$$u_s = G^{-1}(x)[-\hat{H}(x) + v] \tag{29}$$

$\hat{G}(x)$ is invertible and $v = [v_1 \quad v_2]^T$ is considered the new discontinuous feedback control.

By replacing u_s in (28), the dynamics of Ω and ϕ_r take the following form:

$$\ddot{S} = \left(\Delta H - \Delta G\, \hat{G}^{-1}\hat{H}\right) + \left(1 + \Delta G\hat{G}^{-1}\right)v \tag{30}$$

Assume that the following functions are bounded, $\forall$ v, such as:

$$\begin{matrix} 0 < K_{mi} \leq \left(1 + \Delta G_i\, \hat{G}_i^{-1}\right) \leq K_{Mi} \\ \left|\left(\Delta H_i - \Delta G_i\, \hat{G}_i^{-1}\hat{H}_i\right)\right| < C_{0i} \end{matrix}, \; i = 1, 2 \tag{31}$$

with K_{mi}, K_{Mi}, and C_{0i} being positive constants.

According to (30) and (31), it is possible to apply the previously presented twisting algorithm. The control v is then defined by:

$$v_i = \begin{cases} -\lambda_{mi}\ sgn(S) & if \quad S_i\dot{S}_i \leq 0 \\ -\lambda_{Mi}\ sgn(S) & if \quad S_i\dot{S}_i > 0 \end{cases}, \qquad i = 1,2 \tag{32}$$

Where λ_{mi}, λ_{Mi} are positive constants checking the following conditions:

$$0 < \lambda_{mi} < \lambda_{Mi}, \qquad K_{mi}\lambda_{Mi} - C_{0i} > K_{Mi}\lambda_{mi} + C_{0i}$$

For its implementation, we need the sign of the derivative of the surface $(\dot{S})$, which can either be obtained by the Matlab function (du/dt) or estimated in a time interval by the sign of the expression $S(t) - S(t-\tau)$ where τ is the sampling period.

5. Experimental setup

The presented sliding mode controls are implemented using an experimental configuration that includes an ADC interface board (CP1104) and a Dspace card (DS1104 controller board with TMS320F240 slave CPU). The DC bus voltage is linked to a three-phase VSI inverter with a 10 kHz switching frequency. PWM output channels, encoder inputs, and analog inputs are all included in the experimental setup. The control program is written in Matlab/Simulink real-time interface. The IM used is a three-phase Y-connected four-pole 1.5 kW, 50 Hz, 3.5 A rating. Detailed IM parameters are given in Table 1.

Table 1. Induction motor parameters.

Parameter	Value	Unit
Nominal rate power	1.5	kW
Nominal rotor speed	1140	rpm
Nominal voltage	220/380	V
Rated load	10	Nm
Number of pole pairs p	2	poles
Resistances: Rr, Rs	4.2, 5.72	Ω
Inductances: Lr, Ls	0.462	H
Inductance mutual M	0.4402	H
Inertia moment j	0.0049	kg.m2
Friction coefficient F	0.003	N.m.s

5.1. Presentation of the benchmark

The overall configuration of the control system for IM is shown in Figure 2. All parameters of IM are taken to be known and constant, with the exception of the rotor time constant T_r, which will change while the motor is running.

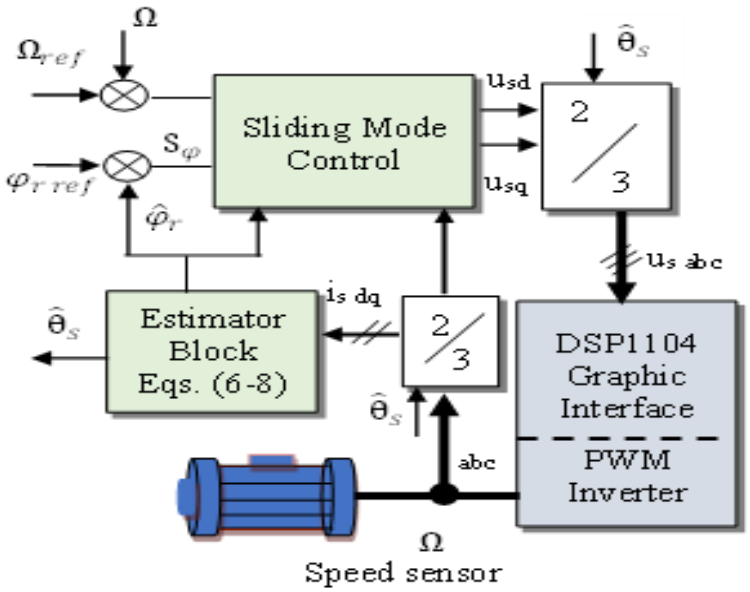

Figure 2. Block diagram of the proposed control scheme.

The two proposed sliding mode vector controls use the measured velocity Ω, estimated flux $\hat{\phi}_r$ given by (6), corresponding position angle $\hat{\theta}_s$ given by (7), and stator current measurements (i_{sd}, i_{sq}). These control inputs control the three-phase inverter, making it possible to impose the monitoring of the flux and speed trajectories. The load torque is imposed on the asynchronous machine by a powder brake powered by a direct current of 0.15 A; the sampling period is $T_e = 10^{-4}s$. The reference speed is applied as soon as the rotor flux is established. 5 Hz is utilized as the low pass filter's cutoff frequency for the measured speed.

The sliding mode control block diagram of the first-order SMC and second-order SMC are shown in Figures 3 and 4, respectively.

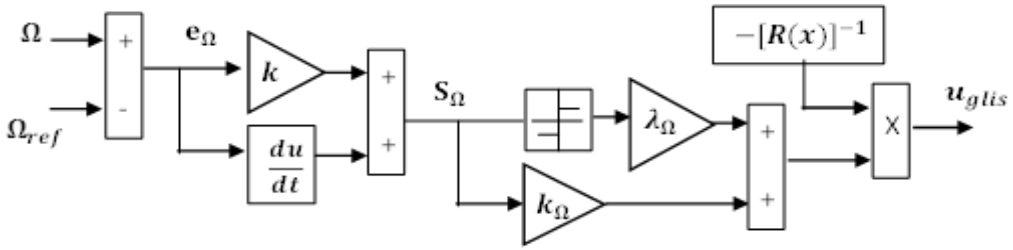

Figure 3. Block diagram of the speed discontinuous control law u_{glis} of the first-order SMC scheme.

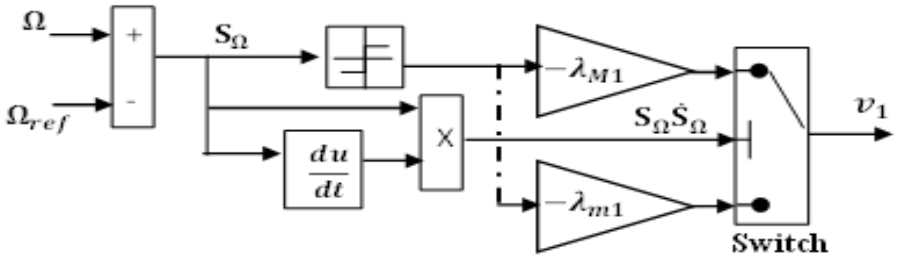

Figure 4. Block diagram of the speed discontinuous control law v_1 of the second-order SMC scheme.

To make a more relevant comparison of the proposed control laws, the speed profiles were designed, allowing us to evaluate their performance at variable speeds (low speed, nominal speed, inversed speed), in the presence of the load torque and the variation of the rotor time constant Tr, and to highlight the tracking capabilities of control algorithms at different regimes. Figure 5 shows the profiles used during the experimental tests. The criteria for comparing control laws include the quality of the transition regime response and the ability to track various speed references under conditions of load torque and parameter variations.

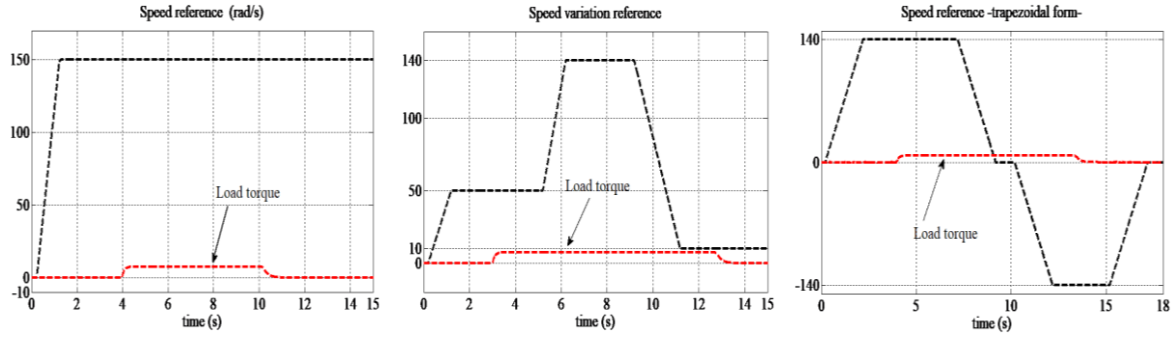

Figure 5. Reference profiles used for different speed control tests.

5.2. Experimental results of the implemented controls

To compare and confirm the efficacy of the suggested first- and second-order sliding mode controls under the same conditions, several experimental findings are given. The response of each method is observed under different operating conditions such as a step change in the load torque, speed variation, and variation of the rotor time constant. The regulation parameters of the second-order SMC used in experimental tests are as follows: speed gain constant, $\lambda_{M1} = 3200$, $\lambda_{m1} = 1000$, rotor flux gain constant, $\lambda_{M2} = 8500$, $\lambda_{m2} = 4000$.

Test 1: Tracking performance

We present the disturbance rejection and evaluate the IM's speed progression. The test is related to the performances of the drive system at 150 rad/s reference speed shown in Figure 5; a load torque of 7.8 Nm is applied from t = 4 s to t = 10 s. Figure 6 shows that speed tracking is very quietly maintained while a proper rejection of the load torque is achieved. Speed and flux responses as well as disturbance rejection are improved by second-order SMC.

The stator current and the stator voltage responses in the synchronous reference frame (d, q) given by Figure 7 show a perfect decoupling between the torque and the rotor flux, with a good reduction of the chattering in the second-order SM control by the twisting algorithm. Stator current components i_{sq} vary proportionally to the applied load torque, presenting the response of the electromagnetic torque.

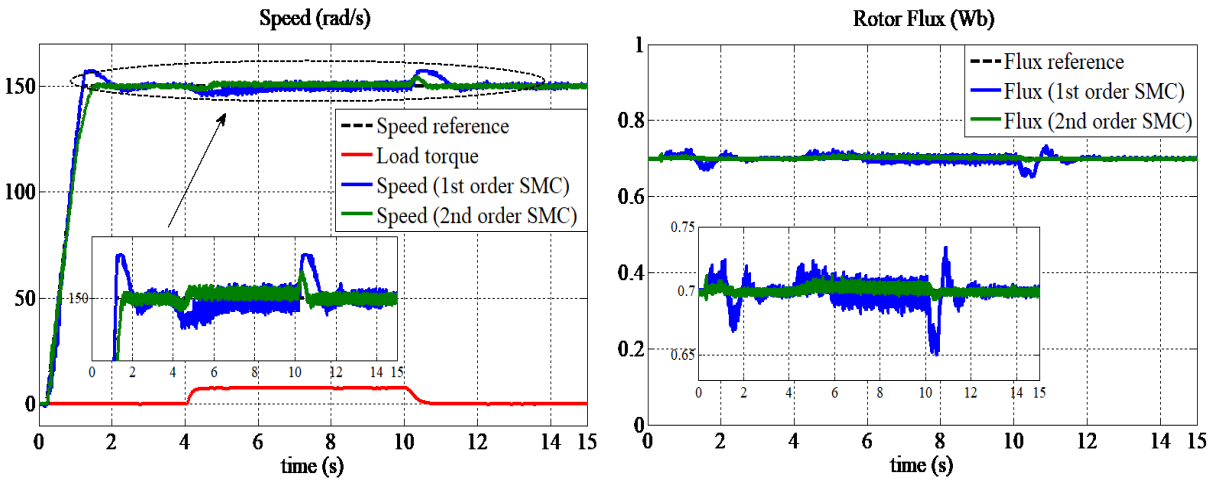

Figure 6. Experimental dynamic responses of speed and rotor flux under load torque T_L = 7.8 Nm. Comparison between the two responses of first-order and second-order SMC.

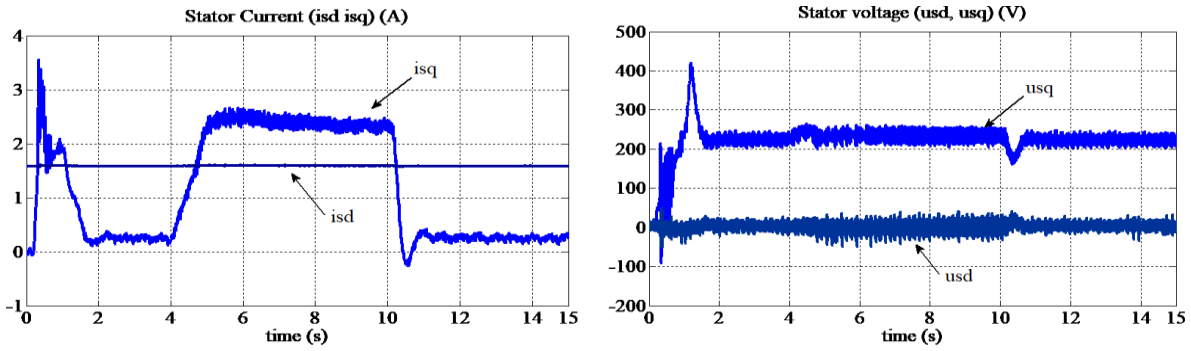

First-order SMC

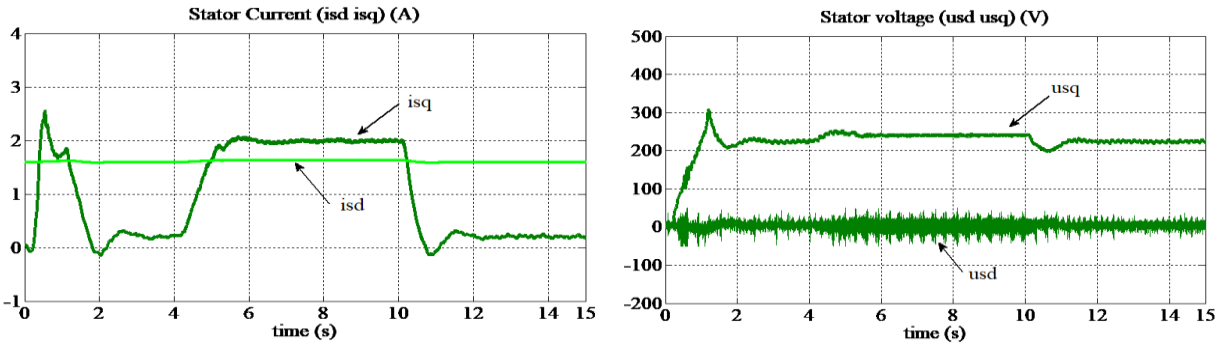

Second-order SMC

Figure 7. Experimental dynamic responses under load torque T_L = 7.8 Nm of stator current and stator voltage in synchronous reference frame.

Test 2: Speed variation

We take into account the speed tracking performances for a broad variety of reference speeds in this test. First, the induction motor is accelerated to 50 rad/s from a standstill; then, it is accelerated again to 140 rad/s and decelerated to a low speed of 10 rad/s. The twisting control algorithm, as shown in Figure 8, illustrates the strong speed tracking and proper rejection of the load torque,

presenting extremely weak oscillations at low speeds compared to the control carried out by the first-order sliding mode.

As seen in Figure 9, the reference speed has been modified to the trapezoidal shape in order to validate speed tracking. It is evident that even in reverse speed operation, the speed converges to the reference trajectory and rejects the load torque rather effectively. Stator voltages $(u_{s\alpha}, u_{s\beta})$ recorded in the stationary reference frame, shown by Figure 9, present a satisfactory response, and the SOSMC control with twisting algorithm improved chattering reduction.

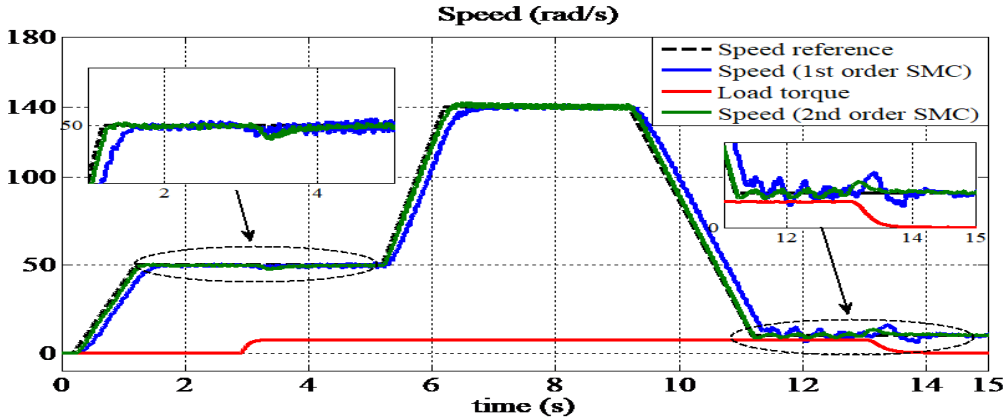

Figure 8. Speed variation under load torque. Comparison between the two speed responses of first-order and second-order SMC.

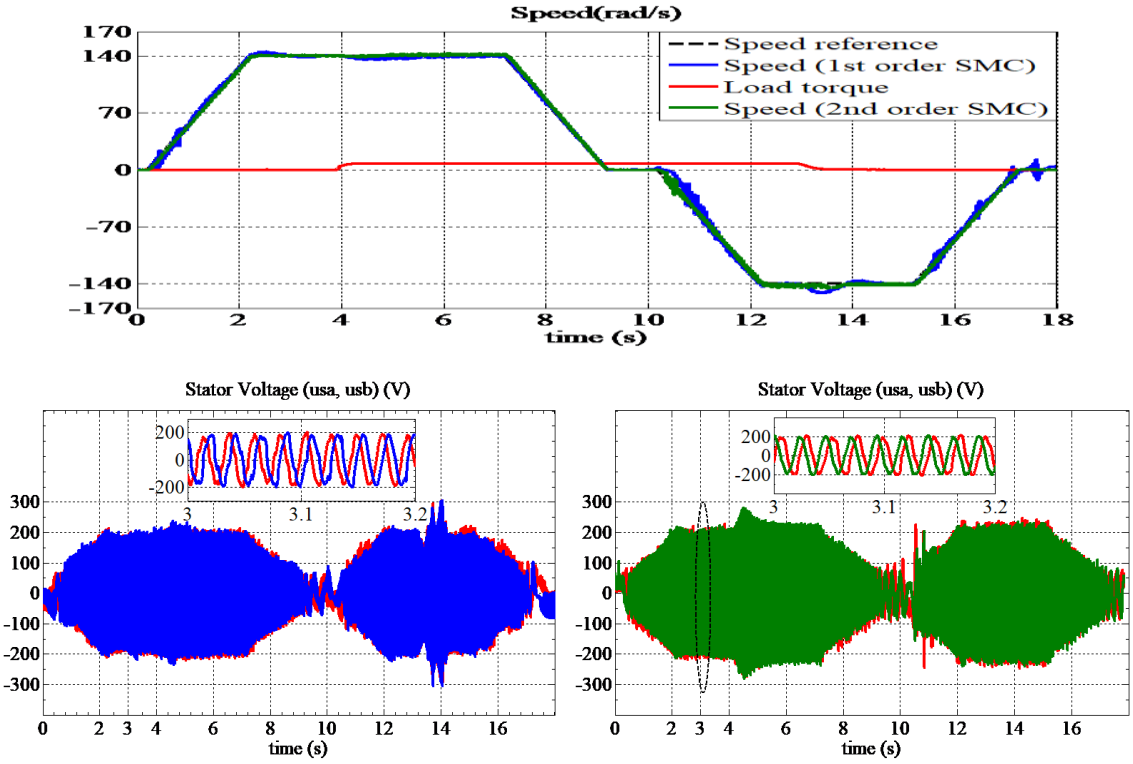

First-order SMC Second-order SMC

Figure 9. Experimental dynamic responses of reverse speed and stator voltage $(u_{s\alpha}, u_{s\beta})$ under load torque T_L = 7.8 Nm.

Test 3: Robustness against parametric variations.

This test was performed to validate and evaluate system performance and robustness against parameter variation. During this test, 100% variation of 1/Tr is taken into account from t = 8.2 s to t = 12.2 s, and the load torque is applied at t = 4 s, as shown in Figure 10. The rotor flux is perfectly oriented on the d-axis, and the load torque is rejected with great efficiency, resulting in superb speed control, no noticeable changes when the torque is increased, and no significant chattering. Results obtained by the second-order SM control are improved compared to those of the first order.

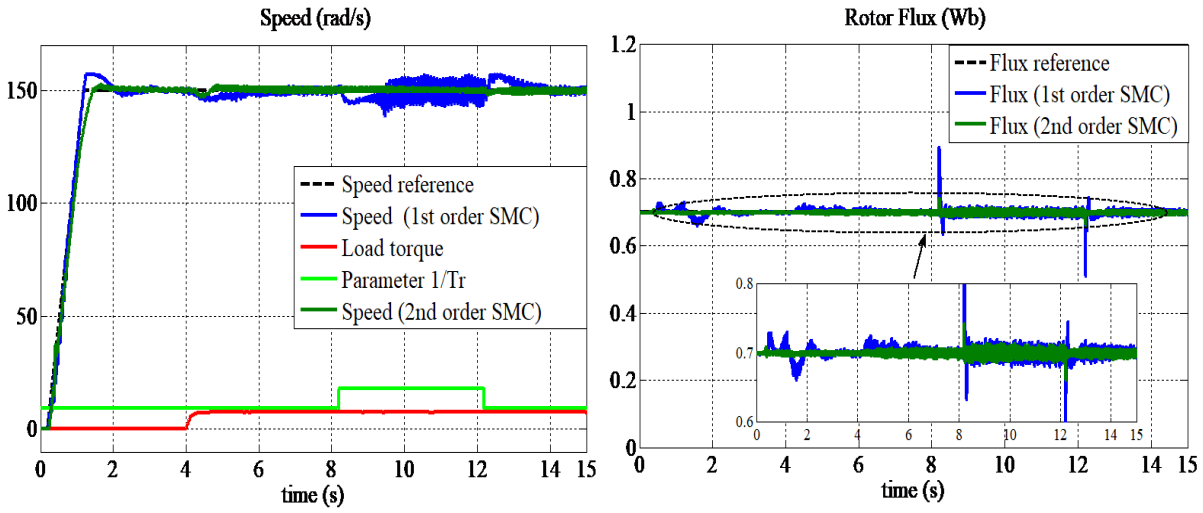

Figure 10. Experimental dynamic responses under load torque TL = 7.8 Nm and 100% variation of 1/Tr.

6. Conclusions

Two sliding mode techniques have been proposed and implemented for speed and rotor flux control of induction motors. Through the results obtained experimentally, the two sliding mode techniques allowed us to synthesize a robust control of the induction motor. Under load and rotor time constant variations, acceleration, deceleration, and speed reversal modes were investigated for speed convergence and speed tracking in various speed ranges. By comparing the first-order and second-order sliding mode control, we discovered that the twisting algorithm achieved smoother speed and rotor flux forms than the first-order sliding mode control. Also, the reduction in ripple in voltage and current responses revealed an improved dynamic performance of the induction motor. We conclude that the second-order sliding mode control reliably decreases chattering under all conditions while still maintaining the advantages of the classical sliding mode control.

Author contributions

Hadda Benderradji: Conceptualization, Software, Investigation, Writing – original draft, Writing – review and editing; Samira Benaicha: Writing – original draft; Larbi Chrifi Alaoui: Software, Investigation. All authors have read and agreed to the published version of the manuscript.

Use of AI tools declaration

The authors declared they have not used Artificial Intelligence (AI) tools in the creation of this article.

Conflict of interest

All authors declare no conflicts of interest in this paper.

References

1. Leonhard W (2001) Control of Electrical Drives. *Science and Business Media,* 3rd. Ed., Springer, Berlin, Germany, 2001.
2. Kelemen A, Imecs M (1992) Vector control of induction machine drives, *Ecriture*, Budapest.
3. Blaschke F (1972) The principle of field orientation as applied to the new transvector closed-loop control system for rotating-field machine. *Siemens Review* 34: 217–220.
4. Tran CD, Nguyen TX, Nguyen PD (2021) A field-oriented control method using the virtual currents for the induction motor drive. *International Journal of Power Electronics and Drive Systems* (IJPEDS) 12: 2095–2101. https://doi:10.11591/ijpeds
5. Zellouma D, Bekakra Y, Benbouhenni H (2023) Field-oriented control based on parallel proportional–integral controllers of induction motor drive. *Energy Reports* 9: 4846–4860. https://doi.org/10.1016/j.egyr.2023.04.008
6. Fadhil AH, Lina JR (2024) Combining fractional-order PI controller with field-oriented control based on maximum torque per ampere technique considering iron loss of induction motor. *AIMS Electronics and Electrical Engineering* 8: 370–393. https://10.3934/electreng.2024018
7. Wang F, Mei X, Tao P, Kennel R, Rodriguez J (2017) Predictive field-oriented control for electric drives. *Chinese Journal of Electrical Engineering* 3: 73–78. https://doi.org/10.23919/CJEE.2017.7961324
8. Nordin K B, Novotny DW, Zinger DS (1985) The influence of motor parameter deviations in feedforward field orientation drive systems. *IEEE T Ind Appl* IA-21: 1009–1015. https://doi.org/10.1109/TIA.1985.349571
9. Utkin VI, Guldner J, Shi J (2017) Sliding mode control in electromechanical systems. *Pub. Boca Raton*. 2nd Eds., Taylor-Francis Group. https://doi.org/doi.org/10.1201/9781420065619
10. Saqib JR, Saba J, Yawar R, Mohsin J (2023) Sliding mode control rotor flux MRAS based speed sensorless induction motor traction drive control for electric vehicles. *AIMS Electronics and Electrical Engineering* 7: 354–379. https://doi.10.3934/electreng.2023019
11. Rekha T, Anandita C (2024) An experimental analysis of fuzzy logic-sliding mode based IFOC controlled induction motor drive. *AIMS Electronics and Electrical Engineering* 8: 340–359. https://doi.10.3934/electreng.2024016
12. Kachroo P (1999) Existence of solutions to a class of nonlinear convergent chattering-free sliding mode control systems. *IEEE T automat contr* 44: 1620–1624. https://doi.org/10.1109/9.780438
13. Shyu KK, Shieh HJ (1996) A new switching surface sliding- mode speed control for induction motor drive systems. *IEEE T Power Electr* 11: 660–667. https://doi.org/10.1109/63.506132

14. Shaija PJ, Daniel AE (2021) Robust sliding mode control strategy applied to IFOC induction motor drive. *2021 Fourth International Conference on Electrical, Computer and Communication Technologies, (ICECCT),* 1–6. IEEE. https://doi:10.1109/ICECCT52121.2021.9616948
15. Seshagiri S, Khalil HK (2002) On introducing integral action in sliding mode control. *2002 41st Conference on Decision and Control,* 1473–1478. https://doi.org/10.1109/CDC.2002.1184727
16. Barambones O, Garrido AJ, Maseda FJ (2007) Integral sliding mode controller for induction motor based on field-oriented control theory. *IET Control Theory and Applications* 1: 786–794. https://doi.org/10.1049/iet-cta:20060239
17. Pan Y, Yang C, Pan L, Yu H (2018) Integral sliding mode control: performance, modification, and improvement. *IEEE T Ind Inform* 14: 3087–3096. https://doi.org/10.1109/TII.2017.2761389
18. Yadav SL, Karvekar SS (2022) Design of integral sliding mode controller for speed control of induction motor. *2022 2nd International Conference on Intelligent Technologies,* 1–6. https://doi:10.1109/CONIT55038.2022.9847959
19. Shiravani F, Alkorta P, Cortajarena JA, Barambones O (2022) An enhanced sliding mode speed control for induction motor drives. *Actuators* 11: 18. https://doi.org/10.3390/act11010018
20. Lumertz MM, dos Santos STCA, Guazzelli PRU, de Oliveira CMR, de Aguiar ML, Monteiro JRBDA (2023) Performance-based design of pseudo-sliding mode speed control for electrical motor drives. *Control Eng Pract* 132: 105413. https://doi.org/10.1016/j.conengprac.2022.105413
21. Oliveira CM, Aguiar ML, Monteiro JR, Pereira WC, Paula GT, Almeida TE (2016) Vector control of induction motor using an integral sliding mode controller with anti-windup. *J Control Autom Electr Syst* 27: 169–178. https://doi.org/10.1007/s40313-016-0228-4
22. Fridman L, Levant A (2002) Higher order sliding modes, Higher order sliding modes. *Sliding mode control in engineering* 11: 53–101.
23. Goh KB, Dunnigan MW, Williams BW (2004) Robust chattering-free (higher order) sliding mode control for a vector-controlled induction machine. *2004 5th Asian control conference* 2: 1362–1370.
24. Levant A (1993) Sliding order and sliding accuracy in sliding mode control. *Int J Control* 58: 1247–1263. https://doi.org/10.1080/00207179308923053
25. Levant A (2007) Principles of 2-sliding mode design, *Automatica* 43: 576–586. https://doi.org/10.1016/j.automatica.2006.10.008
26. Bartolini G, Ferrara A, Usai E (1998) Chattering avoidance by second-order sliding mode control. *IEEE T Automat Contr* 43: 241–246. https://doi.org/10.1109/9.661074
27. Bartolini G, Marchesoni M, Pisu P, Usai E (1998) Chattering reduction and robust position control in induction motor with second-order VSS. *Int J Syst Sci* 29: 1–12. https://doi.org/10.1080/00207729808929490
28. Floquet T, Barbot JP, Perruquetti W (2000) Second order sliding mode control for induction motor. *2000 39th Conference on Decision and Control* 2: 1691–1696. https://doi:10.1109/CDC.2000.912105
29. Smaoui M, Brun X, Thomasset D (2005) A combined first and second order sliding mode approach for position and pressure control of an electropneumatic system. *2005 Proceedings of American Control Conference*, 3007–3012. https://doi.org/10.1109/ACC.2005.1470432

30. Farhi SE, Sakri D, Golèa N (2022) High-performance induction motor drive based on adaptive super-twisting sliding mode control approach. *Arch Electr Eng*, 245–263. https://doi.org/10.24425/aee.2022.140208
31. Listwan J (2018) Application of super-twisting sliding mode controllers in direct field-oriented control system of six-phase induction motor: experimental studies. *Power Electronics and Drives* 3: 23–34. https://doi:10.2478/pead-2018-0013
32. Utkin VI, Poznyak AS, Ordaz P (2011) Adaptive super-twist control with minimal chattering effect. *2011 50th IEEE Conference on Decision and Control and European Control Conference*, 7009–7014. https://doi:10.1109/CDC.2011.6160720
33. Ding S, Wang J, Zheng WX (2015) Second-order sliding mode control for nonlinear uncertain systems bounded by positive functions. *IEEE T Ind Electron* 62: 5899–5909. https://doi.org/10.1109/TIE.2015.2448064
34. Filippov AF (1998) Differential equations with discontinuous Right-Hand Side, *Mathematics and Its Applications*, Kluwer Academic, Dordrecht.
35. Saghafinia A, Wooi Ping H, Nasir Uddin M (2014) Fuzzy sliding mode control based on boundary layer theory for chattering-free and robust induction motor drive. *The International Journal of Advanced Manufacturing Technology* 71: 57–68. https://doi.org/10.1007/s00170-013-5398-7

AIMS Press